



Degradation of polyethylene glycols and polypropylene glycols in microcosms simulating a spill of produced water in shallow groundwater

Journal:	<i>Environmental Science: Processes & Impacts</i>
Manuscript ID	EM-ART-06-2018-000291.R1
Article Type:	Paper
Date Submitted by the Author:	31-Aug-2018
Complete List of Authors:	Rogers, Jessica; University of Colorado, Boulder, Civil, Environmental, and Architectural Engineering; S.S. Papadopoulos & Associates, Inc., Thurman, E. Michael; University of Colorado Boulder, Civil, Environmental, and Architectural Engineering Ferrer, Imma; University of Colorado Boulder, Civil, Environmental, and Architectural Engineering Rosenblum, James; University of Colorado Boulder, Civil, Environmental, and Architectural Engineering Evans, Morgan; The Ohio State University, Civil, Environmental, and Geodetic Engineering Mouser, Paula; The Ohio State University, Civil, Environmental, and Geodetic Engineering; University of New Hampshire, Civil and Environmental Engineering Ryan, Joseph; University of Colorado, Boulder, Civil, Environmental, and Architectural Engineering

1
2
3 **Degradation of polyethylene glycols and polypropylene glycols in microcosms simulating a**
4 **spill of produced water in shallow groundwater**
5

6
7 **Jessica D. Rogers^{1,2}, E. Michael Thurman¹, Imma Ferrer¹, James S. Rosenblum¹,**
8 **Morgan V. Evans³, Paula J. Mouser^{3,4}, and Joseph N. Ryan^{1*}**

9 ¹ Department of Civil, Environmental and Architectural Engineering
10 University of Colorado Boulder, Boulder, CO 80309

11 ² S.S Papadopulos & Associates, Inc.; Boulder, CO 80303

12 ³ Department of Civil, Environmental and Geodetic Engineering
13 The Ohio State University, Columbus, OH 43210

14 ⁴ Department of Civil and Environmental Engineering
15 University of New Hampshire, Durham, NH 03824

16
17
18 * Corresponding author, phone: (303)492-0772; e-mail: joseph.ryan@colorado.edu
19
20

21 **ENVIRONMENTAL SIGNIFICANCE STATEMENT**
22

23
24 Given the frequency of surface spills of produced fluids from unconventional oil and gas
25 operations, there is a need to better characterize resulting groundwater contamination. Produced
26 fluids are known have complex and variable chemical and microbial composition that could
27 influence contaminant fate and transport in groundwater; however, studies on the behavior of
28 compounds measured in produced water under environmentally-relevant conditions are limited.
29
30 This study investigates degradation pathways and kinetics of the frequently-used ethoxylated
31 surfactants polyethylene glycol and polypropylene glycol under conditions simulating a release
32 to shallow groundwater of produced water from two hydraulically-fractured oil and gas wells at
33 varying production times. These results may be utilized to better characterize shallow
34 groundwater contamination following a release of produced water.
35
36
37
38
39
40
41
42
43
44
45
46
47
48
49
50
51
52
53
54
55
56
57
58
59
60

1
2
3
4
5
6
7
8
9
10
11
12
13 **Degradation of polyethylene glycols and polypropylene glycols in**
14 **microcosms simulating a spill of produced water in shallow**
15 **groundwater**
16
17
18
19
20
21

22 **Jessica D. Rogers^{1,2}, E. Michael Thurman¹, Imma Ferrer¹, James S. Rosenblum¹,**
23 **Morgan V. Evans³, Paula J. Mouser^{3,4}, and Joseph N. Ryan^{1*}**
24
25
26

27 ¹ Department of Civil, Environmental and Architectural Engineering
28 University of Colorado Boulder, Boulder, CO 80309
29
30

31
32 ² S.S. Papadopulos & Associates, Inc.
33 Boulder, CO 80303
34
35
36

37
38 ³ Department of Civil, Environmental and Geodetic Engineering
39 The Ohio State University, Columbus, OH 43210
40
41

42
43 ⁴ Department of Civil and Environmental Engineering
44 University of New Hampshire, Durham, NH 03824
45
46
47

48
49 * Corresponding author, phone: (303)492-0772

50 e-mail: joseph.ryan@colorado.edu

51 address: 607 UCB, Boulder, CO 80303
52
53
54
55
56
57
58
59
60

ABSTRACT

1
2
3 1
4
5 2 Polyethylene glycols (PEG) and polypropylene glycols (PPG) are frequently used in
6
7 3 hydraulic fracturing fluids and have been detected in water returning to the surface from
8
9 4 hydraulically-fractured oil and gas wells in multiple basins. We identified degradation pathways
10
11 5 and kinetics for PEGs and PPGs under conditions simulating a spill of produced water to shallow
12
13 6 groundwater. Sediment-groundwater microcosm experiments were conducted using four
14
15 7 produced water samples from two Denver-Julesburg Basin wells at early and late production.
16
17 8 High-resolution mass spectrometry was used to identify the formation of mono- and
18
19 9 di-carboxylated PEGs and mono-carboxylated PPGs, which are products of PEG and PPG
20
21 10 biodegradation, respectively. Under oxic conditions, first-order half-lives were more rapid for
22
23 11 PEG (<0.4-1.1 d) compared to PPG (2.5-14 d). PEG and PPG degradation corresponded to
24
25 12 increased relative abundance of primary alcohol dehydrogenase genes predicted from
26
27 13 metagenome analysis of the 16S rRNA gene. Further degradation was not observed under
28
29 14 anoxic conditions. Our results provide insight to the differences between degradation rates and
30
31 15 pathways of PEGs and PPGs, which may be utilized to better characterize shallow groundwater
32
33 16 contamination following a release of produced water.
34
35
36
37
38
39
40
41
42
43
44
45
46
47
48
49
50
51
52
53
54
55
56
57
58
59
60

17 INTRODUCTION

18 The combined technologies of horizontal drilling and hydraulic fracturing have facilitated
19 rapid expansion of unconventional oil and gas development, raising a number of public concerns
20 including the introduction of chemicals used in hydraulic fracturing fluids to the environment.¹⁻³
21 Hydraulic fracturing fluids are pumped into low-permeability hydrocarbon-bearing formations at
22 high pressures to enhance well production. A typical fracturing fluid is composed of about 90%
23 water, 9% sand, and 0.5–3% chemical additives.⁴⁻⁶ Following well stimulation, the fracturing
24 fluids along with formation brines are co-produced with the hydrocarbons, referenced herein as
25 “produced water.” Recent studies and advances in analytical methods have improved knowledge
26 of the composition of produced water,⁷⁻⁹ which has been shown to vary between different wells,
27 formations, and production ages.⁸⁻¹¹

28 Several studies have reported groundwater contamination linked to known or suspected
29 releases of oil- and gas-related fluids.¹²⁻¹⁴ In the Denver-Julesburg Basin in northeastern
30 Colorado, the number of reported surface spills that contaminated shallow groundwater with one
31 or more of benzene, toluene, ethylbenzene, and xylenes increased from about 60 to 100 spills
32 annually between 2007 and 2014.¹⁵ Produced water has been reported as one the most
33 frequently-released materials in most major United States unconventional resource plays.^{16, 17}
34 Given the frequency of accidental surface spills, there is a need to understand the natural
35 attenuation rates and pathways of organic constituents identified in the produced fluids.

36 Homologous series of polyethylene glycols (PEG) and polypropylene glycols (PPG) have
37 been detected in produced water from multiple basins.¹⁸⁻²² PEGs and PPGs are frequently
38 reported as constituents in fracturing fluid additives including surfactants, emulsifiers, and
39 crosslinkers.^{5, 6, 23} A recent study of the temporal evolution of produced water composition in the

1
2
3 40 Denver-Julesburg Basin showed that PEGs and PPGs were present after 400 days of
4
5 41 production.¹¹ PEGs and PPGs have been suggested as potential environmental tracers because
6
7 42 they have been frequently reported in produced water and are present from the injected fluids as
8
9 43 opposed to being natural constituents of the formation brines.^{11, 19}

12 44 Recent studies have shown biodegradation to be an important removal mechanism for
13
14 45 some organic compounds identified in fracturing fluids and produced waters under
15
16 46 environmentally-relevant conditions.²⁴⁻²⁸ PEGs have been reported as rapidly biodegraded under
17
18 47 aerobic conditions.²⁸⁻³¹ While PPGs have also been found to be biodegradable under aerobic
19
20 48 conditions,^{29, 31-33} they have been shown to be more persistent than PEGs.^{29, 31} Under aerobic
21
22 49 conditions, both PEGs and PPGs are biotransformed through stepwise shortening of terminal
23
24 50 primary alcohol groups via alcohol and aldehyde dehydrogenase enzymatic pathways in
25
26 51 succession, producing carboxylated intermediates.^{34, 35} Anaerobically, PEGs are biodegraded via
27
28 52 the diol dehydratase pathway,³⁶ while PPGs have been shown to be more recalcitrant under
29
30 53 anoxic conditions.³⁶⁻³⁸ Given their relatively hydrophilic nature, PEGs and PPGs are expected to
31
32 54 be fairly mobile in groundwater.

35
36
37 55 Our objective was to measure degradation pathways and kinetics for PEGs and PPGs
38
39 56 under conditions simulating a release of produced waters to shallow groundwater. Produced
40
41 57 water chemical and microbiological composition varies between different wells and production
42
43 58 ages;^{10, 11} thus, sediment-groundwater microcosm experiments were conducted using four
44
45 59 produced water samples from two Denver-Julesburg Basin wells at early and late production.
46
47 60 High resolution mass spectrometry was complemented by analysis of microbial community
48
49 61 dynamics and predictive metagenomics analysis to investigate PEG and PPG degradation
50
51 62 pathways and kinetics.
52
53
54
55
56
57
58
59
60

METHODS

64 Produced water samples

65 Four produced water samples were collected from two horizontal wells (referenced as
66 wells “A” and “B”) targeting the Niobrara Formation in the Denver-Julesburg Basin in Weld
67 County, Colorado. Both wells were hydraulically fractured with gel-based treatments (Tables S1
68 and S2). Samples were collected from each well at early and late production times. Early time
69 samples were collected 22 d after production began from well A (“A-22”) and 14 d after
70 production began from well B (“B-14”). Late time samples were collected 611 d after
71 production began from well A (“A-611”) and 161 d after production began from well B
72 (“B-161”). All samples were collected from the gas/oil/water separator in pre-baked 4 L amber
73 glass jugs with no headspace, and stored at 4°C.

75 Aquifer material and groundwater composition

76 Sediments were collected via hand auger between the depths of 0.9 m (depth of the water
77 table) and 2.5 m from an alluvial aquifer adjacent to the South Platte River in the
78 Denver-Julesburg Basin. The formation is characterized as unconsolidated, coarse-grain sand
79 and gravel with interbedded clays in some areas.³⁹ Collected sediments were homogenized,
80 sieved through a 2 mm mesh, and stored saturated with native groundwater at 4°C (details in
81 Supporting Information). Sieved sediments were composed of well-graded sand, with an organic
82 carbon content of 0.37% w/w (Table S3).

83 During a release, spilled fluids mix with shallow groundwater; thus, the produced water
84 was diluted with a synthetic groundwater representative of Denver-Julesburg Basin surficial
85 aquifers with respect to major ions and pH (details in SI). The synthetic groundwater was

1
2
3 86 dominated by sodium and sulfate with a pH of 7.5 (Table S3). Dilution factors ranged from
4
5 87 7-12 \times and were determined by normalizing the initial benzene concentration in the microcosms
6
7
8 88 to 1 mg L⁻¹, which was representative of groundwater concentrations measured immediately
9
10 89 following surface spills of produced water in the Denver-Julesburg Basin (details on spills
11
12 90 analysis provided in SI).

13 91

14 15 16 17 92 **Microcosm experiments**

18
19 93 Microcosm experiments were conducted using sacrificial sampling. Individual
20
21 94 microcosms were constructed by diluting the produced water with synthetic groundwater (7-12 \times)
22
23 95 and adding 100 mL of the mixture to 125 mL pre-baked borosilicate glass serum bottles with
24
25 96 25 g of saturated sediments (1:5 solids-to-liquids ratio). Abiotic control microcosms were
26
27 97 prepared for each produced water by adding 5.0 g L⁻¹ sodium azide to the synthetic groundwater
28
29 98 (NaN₃, \geq 99%, Amresco). For each produced water treatment, triplicates (biotic) or duplicates
30
31 99 (abiotic controls) were sacrificed at every time point. The serum bottles were sealed with
32
33
34
35 100 PTFE-lined septa with a 10% v/v regular atmosphere headspace, which allowed the microcosms
36
37
38 101 to progress from initially oxic to more reducing conditions. Bottles were mixed continuously on
39
40 102 an orbital shaker (100 rpm) in the dark at 21 \pm 1 $^{\circ}$ C.

41
42 103 Microcosm samples were collected using sterile needles and glass syringes. Dissolved
43
44 104 oxygen (DO) and pH were measured immediately using a luminescent dissolved oxygen probe
45
46 105 (LDO101, Hach) and a pH electrode (PHC301, Hach). DO was considered depleted at 1.5 mg L⁻¹
47
48 106 due to the sampling procedure; it was not possible to eliminate all opportunities for
49
50
51 107 re-oxygenation of the sample. Samples for major anions and cations analysis were syringe-
52
53
54 108 filtered (0.2 μ m, polyethersulfone membrane, Pall Corporation). Cation samples were preserved

1
2
3 109 with 1% nitric acid and analyzed using inductively coupled plasma-optical emission
4
5 110 spectroscopy (model 3410+, Applied Research Laboratories). Anions were analyzed by ion
6
7 111 chromatography (model 4500I, Dionex). Suspended and attached adenosine triphosphate (ATP)
8
9 112 was measured using a luminescence assay and luminometer (PhotonMaster, LuminUltra).
10
11 113 Method details for ion and ATP analysis are provided in the SI. Total dissolved solids (TDS)
12
13 114 were analyzed using Standard Method 2540C.⁴⁰ Samples collected for PEG and PPG analysis
14
15 115 were filtered through surfactant-free syringe filters¹⁸ (0.2 μm , PTFE membrane, Pall
16
17 116 Corporation) and stored at 4°C in 2 mL amber glass vials. Sediment samples from a subset of the
18
19 117 A-22 and A-611 (d 0, 1, 3, 21, 49, 86) and B-14 (d 0, 1, 4, 20, 47, 90) microcosms in addition to
20
21 118 samples of the aquifer sediments prior to exposure to the produced water were collected and
22
23 119 stored in 15 mL sterile, RNase- and DNase-free centrifuge tubes at -80°C for microbial
24
25 120 community analysis.
26
27
28
29
30
31
32

33 122 **PEG and PPG identification and analysis**

34
35 123 Identification of PEGs, PPGs, and degradation products was conducted by accurate mass
36
37 124 analysis using ultra high-performance liquid chromatography quadrupole time-of-flight mass
38
39 125 spectrometry (UHPLC/qTOF-MS).¹⁹ Analytes were separated using an UHPLC system
40
41 126 (Series 1290, Agilent Technologies) equipped with a reversed-phase C₈ analytical column
42
43 127 (150 mm x 4.6 mm, 3.5 μm particle size; Zorbax Eclipse XDB-C8, Agilent Technologies),
44
45 128 sample volume of 20 μL , and mobile phases A and B of 0.1% formic acid in water and
46
47 129 acetonitrile, respectively, at a flow rate of 0.6 mL min⁻¹. The initial mobile phase composition
48
49 130 (10% B) was held constant for 5 min, followed by a linear gradient to 100% B after 30 min. A
50
51 131 10 min post-run time was used after each analysis. The UHPLC system was connected to a
52
53
54
55
56
57
58
59
60

1
2
3 132 qTOF-MS (Model 6545, Agilent Technologies) operating in positive ion mode. Accurate mass
4
5 133 spectra were recorded across 50-1000 m/z at 2GHz in full-spectrum mode, and data were
6
7 134 processed with MassHunter software. MS-MS was used to identify selected compounds
8
9 135 (isolation width of $\sim 4 m/z$ and collision energies of 10, 20, and 40 eV). Analytical standards are
10
11 136 only available for mixtures of PEG and PPG homologous and not individual compounds, and
12
13 137 ionization efficiencies may not be the same for all homologues.^{8, 11} Thus, concentrations in
14
15 138 day 0 microcosm samples were estimated from 1 mg L⁻¹ PEG-400 and PPG-425 standards
16
17 139 (polydispersal mixtures of PEG and PPG with average molecular weights of 400 and 425,
18
19 140 respectively; Sigma-Aldrich), using the total response of all homologues. PEGs, PPGs, and
20
21 141 identified products were semi-quantified by comparing the integrated response of each
22
23 142 homologue detected in the microcosm samples to the corresponding homologues measured in the
24
25 143 day 0 microcosm sample.

26
27 144 Following identification of PEGs, PPGs, and products by accurate mass analysis, high-
28
29 145 performance liquid chromatography mass spectrometry (HPLC/MS) was used to semi-quantify
30
31 146 PEG and PPG concentrations to estimate removal kinetics. Analytes were separated at 25°C
32
33 147 using an HPLC system (Series 1100, Agilent Technologies) equipped with an analytical column
34
35 148 as described above. The mobile phase composition was identical to the UHPLC/qTOF-MS
36
37 149 method with a flow rate of 0.4 mL min⁻¹ and an increased sample injection volume of 40 μ L.
38
39 150 The HPLC system was connected to an ion trap MS (LC-MSD Trap XCT Plus, Agilent
40
41 151 Technologies) using electrospray ionization (ESI) operating in full-scan, positive ion mode (m/z
42
43 152 scan range 50-1000). Pseudo-first-order removal rate coefficients were estimated by linear
44
45 153 regression using OriginPro 2016 for the period of observed rapid removal (e.g., within the linear
46
47 154 range).

155 DNA extraction, sequencing, and bioinformatics analysis

156 Total nucleic acids were extracted in replicate from 0.25 g of homogenized sediment
157 slurry using the DNeasy PowerSoil Kit (Qiagen). Triplicate replicates were extracted for all
158 A-22, A-611, and B-14 microcosm sediment samples except day 0 (extracted in singlet) and
159 aquifer sediment samples (extracted in duplicate). Sediment samples from the B-161
160 microcosms were not analyzed for microbial community analysis. DNA was quantified and
161 quality checked using a NanoDrop 2000 (Thermo Fisher Scientific), and the polymerase chain
162 reaction (PCR) amplification of the appropriate sized template was checked prior to sequencing.
163 Library prep and amplification of the V4 region of the 16S rRNA gene was performed at
164 Argonne National Lab according to previously established protocol⁴¹ using primers 515F-806R.
165 The 16S rRNA iTag sequence data were obtained by an Illumina MiSeq at Argonne National
166 Lab. Sequences were processed using the QIIME 1.9.1 pipeline and Ohio Supercomputer^{42, 43}
167 using closed reference operational taxonomic unit (OTU) picking against the GreenGenes
168 database (v.13.8)⁴⁴ with BLASTn and QIIME parameters set at 97% similarity.⁴² An OTU table
169 was generated using taxonomic assignments from BLAST⁴⁵ for all statistical analyses.
170 Rarefaction curves were generated to evaluate sequencing depth (Fig. S1 and S2) and alpha
171 diversity indices were generated in QIIME. After removal of singlets, the OTU table was
172 submitted to the Galaxy portal of the Langille Lab (v.1.1.1) for PICRUSt analysis for predictive
173 metagenome analysis from the 16S rRNA gene.⁴⁶ Gene abundances of primary alcohol
174 dehydrogenase genes (PA-DH, KEGG Orthology identifier K00114)⁴⁷ and anaerobic diol
175 dehydratase genes (*pduC*, K01699)³⁶ were normalized to copies of a housekeeping gene, *recA*
176 (K03553), to account for fluctuations in the number of predicted metagenomes through time and
177 genomes present but lacking functional genes of interest (Fig. S3).^{36, 48} PICRUSt has been

1
2
3 178 shown to yield accurate predictions based on small numbers of 16S rRNA gene sequences across
4
5 179 a breadth of environmental systems.⁴⁶ Statistical testing was performed using R (v.3.4.3). The
6
7
8 180 16S rRNA gene sequences were submitted to the NCBI database and are available under
9
10 181 BioProject ID PRJNA445449.
11

12 182

13 14 15 183 **RESULTS AND DISCUSSION**

16 17 184 **Microcosm water chemistry**

18
19 185 The microcosms were initially oxic and progressed to more reducing conditions. The
20
21 186 oxic/anoxic transition was rapid for the A-22 and B-14 microcosms (3 and 4 d, respectively), and
22
23 187 slower for the A-611 and B-161 microcosms (21 and 28 d, respectively; Fig. 1). In all
24
25 188 biologically-active microcosms, oxygen and nitrate were simultaneously depleted; thus, the oxic
26
27 189 period consisted of mixed oxygen- and nitrate-reducing conditions (Figs. S4-S7). Following the
28
29 190 oxic/anoxic transition, the different microcosms progressed to more reducing conditions, with
30
31 191 final conditions ranging from mixed manganese- and iron-reducing (A-611 and B-161
32
33 192 microcosms) to sulfate-reducing (A-22 and B-14). In the abiotic control microcosms, dissolved
34
35 193 oxygen remained approximately saturated throughout the experiment, and no significant changes
36
37 194 were observed in the concentrations of any redox-active species (Figs. S4-S7). TDS
38
39 195 concentrations in the microcosms were relatively low (1,920-3,260 mg L⁻¹, Table S7). In all
40
41 196 microcosms, the pH quickly dropped from approximately 7.5 to 7.0, and subsequently remained
42
43 197 steady throughout the experiment (Fig. S8).

44
45 198 In all biotic microcosms, ATP production rapidly increased during the oxic period
46
47 199 (Fig. S9). Under oxic conditions, a sharp increase to 10¹⁰-10¹¹ pg total ATP (suspended and
48
49 200 attached) occurred within the first 2 d for all waters. Following the oxic/anoxic transition, total
50
51
52
53
54
55
56
57
58
59
60

1
2
3 201 ATP in the A-22 and B-14 microcosms rapidly declined by two orders of magnitude, after which
4
5 202 ATP concentrations remained steady throughout the remainder of the experiment. In both the
6
7
8 203 A-611 and B-161 microcosms, the initial ATP peak was followed by a steady decline to
9
10 204 approximately 10^7 pg total ATP. For all produced water treatments, ATP concentrations in the
11
12 205 abiotic control microcosms were at least two orders of magnitude lower than in the
13
14
15 206 corresponding biotic microcosms. Rapid ATP production which corresponded to distinct redox
16
17 207 transitions indicate significant microbial activity in the biotic microcosms.
18

19 208
20

21 209 **Identification and transformation products**

22
23
24 210 *Polyethylene glycols (PEGs)*. PEGs were identified by accurate mass analysis. The
25
26 211 average measured mass difference between PEG homologues was 44.0262 u, which represents
27
28 212 the addition of one ethylene oxide unit ($-\text{CH}_2\text{CH}_2\text{-O}-$).¹⁹ Series of PEG homologues with three
29
30
31 213 to fourteen ethylene oxide units were detected in all four produced water samples (Fig. 2;
32
33 214 Table S8).

34
35 215 The relative abundance of shorter chain PEGs was greater in the initial distribution of the
36
37 216 PEG series detected in the A-22 day 0 microcosm relative to the B-14 day 0 microcosm
38
39
40 217 (Fig. 2a,c). The initial distribution of PEGs was nearly identical in A-22 and A-611 (Fig. 2a,b);
41
42 218 however, there was a shift towards shorter chains in B-161 compared to B-14 (Fig 2c,d). The
43
44
45 219 estimated total concentration of all PEG homologues in the A-22 day 0 microcosm was in the
46
47 220 mg L^{-1} range and was approximately an order of magnitude greater than the B-14 day 0
48
49 221 microcosm. Differences in initial PEG distributions and concentrations between the two wells
50
51 222 were likely due to varying fracturing fluid composition. The FracFocus Chemical Disclosure
52
53
54 223 Registry⁴⁹ report for well A listed PEG as an ingredient. Well B's FracFocus report listed a
55
56
57
58
59
60

1
2
3 224 proprietary “surfactant blend” and did not specifically report the use of PEGs (Tables S1 and
4
5 225 S2). Downhole reactions could explain the distribution differences between the two production
6
7 226 ages in well B. Based on hydrophobicity, sorption to the hydrocarbon formation would not be a
8
9 227 significant downhole removal mechanism for the relatively short-chained PEGs returning to the
10
11 228 surface.¹⁸ ATP concentrations indicated biological activity in the produced water collected from
12
13 229 B-14 (8,010 pg L⁻¹ suspended ATP), while ATP concentrations were approximately 3 orders of
14
15 230 magnitude lower in the A-22 produced water sample (10 pg L⁻¹ suspended ATP). Thus,
16
17 231 downhole biodegradation could have occurred in well B, but low biomass activity suggests that
18
19 232 downhole biodegradation was unlikely in well A. Shifts to smaller homologues have been
20
21 233 reported during PEG biodegradation,^{29,30} which could explain the distribution differences
22
23 234 between B-14 and B-161.

24
25
26
27
28 235 After day 1 of the microcosm experiment, chromatographic peaks separated by 44.0262 u
29
30 236 (one ethylene oxide group) were observed eluting approximately 0.5 min later than the detected
31
32 237 PEGs (Fig. 3). The peak at 11.4 min had a measured mass of 460.2396 with companion adducts
33
34 238 at m/z 465.1947 and 443.2126 (Fig. S10). Based on mass differences, the ions were identified as
35
36 239 the ammonium, sodium, and proton adducts, respectively. Figure S10 also shows ions at
37
38 240 m/z 487.1764 and 509.1582, which are 21.9815 and 43.9635 greater than the single sodium
39
40 241 adduct, respectively. The mass difference equates to the addition of a sodium ion minus a
41
42 242 proton, indicating the presence of double (m/z 487.1764) and triple (m/z 509.1582) sodium
43
44 243 adducts. Accurate mass putatively identified a formula of C₁₈H₃₄O₁₂Na⁺ (single sodium adduct)
45
46 244 with a calculated exact mass of m/z 465.1942, which is within 1.1 ppm of the measured mass.
47
48 245 The compound was putatively identified as a di-carboxylated PEG (PEG-diCOOH). The double
49
50 246 and triple sodium adducts occur when one or both carboxyl groups, respectively, are in the form
51
52
53
54
55
56
57
58
59
60

1
2
3 247 of a sodium salt. MS-MS was conducted (details in S2.1; Fig. S11); however, a standard of the
4
5 248 putative PEG-diCOOH product was not available, thus the identification remains unconfirmed.
6
7 249 Mono-carboxylated PEGs (PEG-COOH) were also identified by accurate mass analysis (e.g.,
8
9 250 peak at 11.1 min apparent in Fig. 3b). Single carboxylated PEGs have been previously reported
10
11 251 in produced waters.¹⁹ The small increase in retention time for the carboxylated products
12
13 252 (Fig. 3b) can be explained by the slightly greater hydrophobicity of protonated PEG-COOH and
14
15 253 PEG-diCOOH compared to the parent PEG in the acidic mobile phase in addition to increasing
16
17 254 molecular weights (+14 u) of the carboxylated products. Thurman et al.^{18, 19} demonstrated via
18
19 255 the Kendrick mass scale that for homologous series of ethoxylates it is only necessary to identify
20
21 256 the structure of one homologue in the series, and that the remaining compounds represent the
22
23 257 addition of ethylene oxide units. Thus, accurate-mass analysis presented for the di-carboxylated
24
25 258 product of example homologue PEG-9 (Fig. S10) and the MS-MS analysis conducted for the
26
27 259 example homologue PEG-6-diCOOH (e.g., Fig. S11) apply to the identification of all PEG
28
29 260 homologues in the series. Both PEG-COOH and PEG-diCOOH with four to fourteen ethylene
30
31 261 oxide units were detected in all of the microcosms (Table S8).

32
33 262 PEG-COOH was detected in the day 0 microcosm samples with an integrated response
34
35 263 that was 4-22% of the corresponding PEG; however, PEG-diCOOH was not observed until after
36
37 264 day 1 of the microcosm experiments (Fig. 3c). Both compounds are known PEG biodegradation
38
39 265 intermediates under aerobic conditions.³⁴ In the presence of oxygen, PEGs are enzymatically
40
41 266 altered through oxidation of the terminal primary alcohol group (Fig. 3d), followed by cleavage
42
43 267 of the terminal ether bonds to produce a shorter-chained PEG with two fewer ethylene oxide
44
45 268 units.^{34, 35} The detection of PEG-COOH in the day 0 microcosm sample suggests it may be
46
47 269 present initially as an impurity in the industrial surfactant mixture used in the fracturing fluid or
48
49
50
51
52
53
54
55
56
57
58
59
60

1
2
3 270 formed under downhole conditions.¹⁹ Nevertheless, the increasing response of PEG-COOH with
4
5 271 time and the emergence of PEG-diCOOH (not present at day 0) in conjunction with the removal
6
7 272 of the corresponding PEG provides strong evidence of further formation of the carboxylated
8
9
10 273 products in the microcosms (Fig. 3). Mass spectrometry analysis was not conducted for abiotic
11
12 274 control samples due to high sodium azide concentrations used to inhibit microbial activity; thus,
13
14 275 information needed to distinguish abiotic and biotic removal mechanisms was not obtained.
15
16
17 276 Significant abiotic removal of PEGs has not been reported;²⁸ therefore, PEG transformation and
18
19 277 removal observed in the microcosms was almost surely a result of biodegradation.
20
21
22 278

23
24 279 *Polypropylene glycols (PPGs)*. PPGs were also identified by accurate mass analysis. The
25
26 280 average measured mass difference between PPG homologues was 58.0419 u, which represents
27
28 281 the addition of one propylene oxide unit (-CH₂CH(CH₃)-O-).¹⁹ Series of PPG homologues
29
30 282 ranging from two to ten propylene oxide units were detected in all four produced water samples
31
32
33 283 (Fig. 4; Table S9).

34
35 284 There was greater relative abundance of shorter chain PPGs in the initial distribution of
36
37 285 the PPG series present the A-22 day 0 microcosm compared to the B-14 day 0 microcosm
38
39 286 (Fig. 4a,c). The initial PPG distribution was shifted towards shorter chains in the A-611 and
40
41
42 287 B-161 microcosms (Fig. 4b,d) compared to A-22 and B-14, respectively. The estimated total
43
44 288 PPG concentration was in the range of hundreds of $\mu\text{g L}^{-1}$ and was approximately an order of
45
46 289 magnitude lower in the A-22 day 0 microcosm compared to B-14. The differences in initial PPG
47
48
49 290 distributions and concentrations between the two wells and production times could be due to
50
51 291 both varying fracturing fluid composition and downhole reactions including shale interactions.
52
53
54 292 FracFocus reports from both wells cited proprietary “surfactant blends,” but PPG or blends of
55
56
57
58
59
60

1
2
3 293 ethoxylated surfactants were not specifically identified on either report. PPGs are more
4
5 294 hydrophobic than PEGs;¹¹ thus, sorption of longer-chained PPGs to the hydrocarbon formation
6
7 295 or partitioning to the oil phase could contribute to the shift towards shorter-chained homologues
8
9 296 observed at later production times. Sorption of longer-chained PPGs could explain the similar
10
11 297 initial distributions observed in both the A-611 and B-161 day 0 microcosms.

12
13
14
15 298 After day 1 of the microcosm experiment, chromatographic peaks separated by 58.0419 u
16
17 299 (one propylene oxide group) were observed approximately 0.2 min after the detected PPGs.

18
19 300 With the same approach used to identify PEG-diCOOH, sodium (m/z 403.2302), proton
20
21 301 (m/z 381.2483), and ammonium (m/z 398.2749) adducts were measured for the peak from
22
23 302 16.0-16.6 min (Fig. S12). Accurate mass putatively identified a formula of $C_{18}H_{36}O_8Na^+$
24
25 303 (sodium adduct) with a calculated exact mass of m/z 403.2302, which was an exact match to the
26
27 304 measured mass. The compound was putatively identified as a mono-carboxylated PPG
28
29 305 (PPG-COOH). Analogous to the PEG carboxylates, a double sodium adduct indicated that the
30
31 306 sodium salt of the carboxyl group was present, albeit at trace levels (m/z 425.2129; Fig. S12).
32
33 307 MS-MS was conducted using PPG-7-COOH as an example homologue (details in S2.2;
34
35 308 Fig. S13). The chromatograph of PPG-4 is shown in Figure 5 because numerous isomers are
36
37 309 discernable for relatively short-chained PPGs (see discussion below). PPG-COOH with three to
38
39 310 ten propylene oxide units were identified (Table S9).

40
41
42 311 PPG-COOH was not detected in the day 0 microcosms (Fig. 5). A similar aerobic
43
44 312 metabolic pathway as PEG has been reported for PPG: oxidation of a terminal alcohol (Fig. 5d)
45
46 313 followed by cleavage of the terminal ether bond to produce PPG with one fewer propylene oxide
47
48 314 unit.³²⁻³⁴ The emergence of PPG-COOH corresponding with the removal of PPG demonstrates
49
50 315 that PPG-COOH was formed in the microcosms (Fig. 5). Significant abiotic removal of PPG has
51
52
53
54
55
56
57
58
59
60

1
2
3 316 not been reported;^{33, 36} thus, the transformation and removal observed in the microcosms was
4
5 317 likely a result of biodegradation.

6
7 318 Multiple isomers were apparent for the PPG-COOH product. The number of isomers in
8
9 319 the parent PPG increases exponentially for each additional propylene oxide unit due to
10
11 320 non-symmetric hydroxyl groups on the monomer.^{19, 33} For short-chained PPGs, individual
12
13 321 isomers are apparent in the chromatography as distinct peaks with varying intensities. For
14
15 322 instance, at least nine PPG-4 isomers can be discerned within the four readily-apparent peaks,
16
17 323 and at least five isomers were observed for the corresponding PPG-4-COOH (Fig. 5b). The
18
19 324 PPG-4-COOH isomer peaks had slightly different relative intensities compared to PPG-4, which
20
21 325 indicates that different isomers were transformed to varying extents. Variable transformation for
22
23 326 PPG isomers has been previously suggested.^{33, 34}

24
25
26 327 In contrast to PEG, only a singly-carboxylated PPG product was identified. This is likely
27
28 328 caused by the presence of both primary and secondary terminal alcohols in PPG isomers
29
30 329 resulting from the non-symmetric monomer. PEGs are symmetric homopolymers with two
31
32 330 terminal primary alcohol groups, both of which can be oxidized to form PEG-diCOOH. For
33
34 331 PPG, oxidation of the terminal secondary alcohol to a carboxyl is not expected.⁵⁰ Thus, only
35
36 332 PPG isomers with a terminal primary hydroxyl can be degraded to PPG-COOH. The formation
37
38 333 of a ketone product from the terminal secondary hydroxyl has been reported;³² however, we did
39
40 334 not observe a PPG-ketone product in our microcosm experiments.

41
42
43
44
45
46
47 335

48 49 336 **Degradation kinetics**

50
51 337 Semi-quantitative analysis of PEG and PPG degradation was conducted using the
52
53 338 HPLC/MS method. PEG-9 and PPG-6 were selected as an example PEG and PPG homologues,
54
55
56
57
58
59
60

1
2
3 339 respectively, based on relative abundance in the microcosms (Figs. 2 and 4). Figure 6 shows the
4
5 340 relative response of PEG-9 and PPG-6 during the microcosm experiments, including both the
6
7 341 oxic (filled symbols) and anoxic (open symbols) periods.

8
9
10 342 Under mixed oxygen- and nitrate-reducing conditions, PEG-9 was rapidly removed in all
11
12 343 microcosms (Fig. 6a). First-order half-lives were similar between the four microcosms
13
14 344 (Table 1). In the A-22 and B-14 microcosms, the half-lives were 0.4 and 1.1 d, respectively. In
15
16 345 the A-611 and B-161 microcosms, PEG-9 was not detected by the day 1.5 sample; thus, the
17
18 346 half-life was reported as <0.4 d. Under oxic conditions, PPG-6 degradation was faster for water
19
20 347 collected at late production times ($t_{1/2} = 2.7$ and 2.5 d in A-611 and B-161 microcosms,
21
22 348 respectively) compared to early production times ($t_{1/2} = 7.5$ and 14 d in A-22 and B-14
23
24 349 microcosms; Table 1, Fig. 6b). Our measured rates were consistent with PEG and PPG
25
26 350 biodegradation rates reported under oxic conditions for similar initial concentrations and average
27
28 351 molecular weights, by inoculum sources ranging from river water²⁹ to activated sludge.³⁰⁻³²
29
30 352 Notably, the produced water mixture did not significantly inhibit or enhance PEG and PPG
31
32 353 biodegradation compared to studies where these compounds were the only substrate.
33
34 354 Biodegradation inhibition in mixtures of fracturing fluid organic constituents at high
35
36 355 concentrations representative of the injected fluids has been previously reported.^{26, 28}

37
38 356 Under oxic conditions, PPG degradation was both slower and more variable compared to
39
40 357 the degradation of PEG (Fig. 6). While the occurrence of PEG-diCOOH demonstrates that PEGs
41
42 358 can be degraded from both sides of the molecule, the mono-carboxylated PPG was the only PPG
43
44 359 product identified in the microcosms. Thus, PPG was only degraded where a terminal primary
45
46 360 hydroxyl was present and degradation was effectively blocked for isomers with terminal
47
48 361 secondary hydroxyls. This likely contributed to slower degradation kinetics of PPG compared to
49
50
51
52
53
54
55
56
57
58
59
60

1
2
3 362 that of PEG. Differences in initial PPG concentrations may have contributed to the variable PPG
4
5 363 degradation kinetics observed between microcosms because B-14 had both the highest estimated
6
7 364 initial PPG concentration and the slowest degradation. A recent study under anoxic conditions
8
9 365 suggested a concentration inhibitory effect on PPG biodegradation kinetics.³⁶ In our study,
10
11 366 PPG-6 degradation was overall slower than PEG-9, but the relative succession of half-lives for
12
13 367 the different microcosms was the same for both compounds (B-14 >A-22 >A-611 ≈B-161),
14
15 368 which suggests that produced water composition also may have influenced degradation kinetics.
16
17 369 Similar ATP concentrations in all microcosms during the period corresponding to PEG and PPG
18
19 370 oxic degradation (10^{10} - 10^{11} pg total ATP, Fig. S9) suggest comparable levels of overall biomass
20
21 371 activity, and that a non-specific inhibitor such as a biocide likely did not affect the degradation
22
23 372 kinetics. Competitive inhibition from a more labile or preferred carbon source present in the
24
25 373 early-time produced water could have slowed the rate of PEG and PPG degradation relative to
26
27 374 the waters from later production times. This is consistent with the rapid depletion of dissolved
28
29 375 oxygen observed in the A-22 and B-14 microcosms compared to the A-611 and B-161
30
31 376 microcosms (Fig. 1), which could indicate more competition for available electron acceptors.
32
33 377 TDS concentrations greater than $10,000 \text{ mg L}^{-1}$ can inhibit biological activity;⁷ however, TDS
34
35 378 concentrations in the microcosms were below this threshold ($1,920$ - $3,260 \text{ mg L}^{-1}$, Table S7) and
36
37 379 likely did not inhibit degradation.

380 There was no evidence of further PEG or PPG degradation under anoxic conditions. In
381 the A-22 and B-14 microcosms, low levels of PEG-9 remained at the oxic/anoxic transition
382 (Fig. 6a), but no additional removal was observed. In the A-611 and B-161 microcosms, PEG-9
383 was not detected at the oxic/anoxic transition, likely because the longer oxic period allowed for
384 more complete removal. Anaerobic biodegradation of PEGs has been reported at temperatures

1
2
3 385 $\geq 35^{\circ}\text{C}$,^{51, 52} so it is possible that either the anaerobic microbial community in the microcosms
4
5 386 was unable to degrade PEG, or the kinetics were slow enough under ambient temperatures that
6
7 387 no degradation was observed over the 84-86 d anoxic periods. Due to both different degradation
8
9 388 rates and lengths of the oxic period for the four microcosms, varying levels of PPG-6 remained
10
11 389 at the oxic/anoxic transition (Fig. 6b); however, no further removal was observed under anoxic
12
13 390 conditions in any microcosm. Our observations are in agreement with studies that have reported
14
15 391 PPG as recalcitrant under anaerobic conditions, particularly in the presence of microbial
16
17 392 communities which have not been previously exposed to glycols.³⁶⁻³⁸
18
19
20
21
22
23

24 394 **Microbial community dynamics and abundance of primary alcohol dehydrogenase genes**

25
26 395 Analysis of microbial community dynamics and function based on metagenomes
27
28 396 predicted from the 16S rRNA gene provide further insight into the PEG and PPG biodegradation
29
30 397 pathway. After quality filtering and processing, 14,640-77,563 sequences per sample were
31
32 398 obtained (Table S10). One triplicate sample of B-14 day 4 yielded very low sequence counts
33
34 399 (3,010) and was not used in any analysis; therefore, the error bars associated with this sample
35
36 400 represent a range of duplicate values. Exposure to produced water greatly decreased the diversity
37
38 401 of sediment microbial communities: Shannon's diversity index was 10 in the aquifer sediments
39
40 402 prior to exposure to the produced water and dropped to 5-7 by day 3-4 of the microcosm
41
42 403 experiments. Similarly, microbial community richness decreased from over 3,500 OTUs in the
43
44 404 aquifer sediments to 1,300-2,700 OTUs in microcosm sediment samples in 1-4 days.

45
46 405 Using a bioinformatics approach (PICRUSt), we searched for genes known to catalyze
47
48 406 polyglycol chain shortening in metagenomes predicted from 16S rRNA gene sequences. While
49
50 407 specific PEG- and PPG-degrading enzymes have been proposed,^{35, 53} they remain poorly
51
52
53
54
55
56
57
58
59
60

1
2
3 408 characterized. Thus, primary alcohol dehydrogenase genes (PA-DH) were used as a proxy for
4
5 409 polyglycol biotransformation under oxic conditions via terminal alcohol oxidation. PA-DH is
6
7
8 410 found in several taxonomic groups, including *Pseudomonas*, when grown on a wide variety of
9
10 411 alcohols and acts by oxidation of terminal primary hydroxyl groups.⁵⁴

11
12 412 A sharp increase in the abundance of the PA-DH gene relative to the housekeeping gene
13
14 413 *recA* (PA-DH/*recA*) was observed during the first 1-3 days of the A-22, A-611, and B-14
15
16 414 microcosms (Fig. 7), which coincided with the period of rapid PEG and PPG removal (Fig. 6).
17
18 415 In the A-22 and B-14 microcosms, the relative abundance of PA-DH/*recA* initially spiked to
19
20 416 approximately 0.40 normalized gene copies, followed by a decrease to <0.25. The relative
21
22 417 abundance of PA-DH/*recA* in the A-611 microcosms initially increased to 0.52 and remained
23
24 418 elevated for the duration of the microcosm experiment, which is consistent with faster removal
25
26 419 observed in the late-time compared to the early-time produced waters. The prolonged presence
27
28 420 of dissolved oxygen in A-611 microcosms compared to A-22 and B-14 (Fig. 1) also may have
29
30 421 enabled the persistence of microbial taxa capable of encoding PA-DH genes, which are repressed
31
32 422 under reducing conditions. Trace levels of the diol dehydratase gene *pduC*, associated with
33
34 423 polyglycol chain shortening under anaerobic conditions,³⁶ were predicted in the microcosm
35
36 424 samples; however, *pduC* abundance was at least three orders of magnitude less than that of
37
38 425 PA-DH, which is consistent with the limited PEG and PPG removal observed after the
39
40 426 microcosms changed from oxic to anoxic conditions.

41
42 427 *Pseudomonas* became highly enriched in all of the microcosms through time, increasing
43
44 428 from 0.01% of the aquifer sediment community to 50-65% by day 3 and remaining between 20
45
46 429 and 50% of the terminal community in microcosm sediments (Fig. S14). *Pseudomonas* has been
47
48 430 identified in produced fluids as an important member of hydraulically-fractured shale
49
50
51
52
53
54
55
56
57
58
59
60

1
2
3 431 communities⁵⁵⁻⁵⁷ and was enriched during biodegradation of synthetic hydraulic fracturing fluid
4
5 432 in soil-groundwater microcosms.²⁴ Many species of *Pseudomonas* have the enzymatic capacity
6
7 433 to degrade PEGs; therefore, this taxa may contribute to PEG degradation in the microcosms.⁵⁸⁻⁶¹
8
9 434 The genus *Syntrophobotulus* was also detected, a taxa notable for fermenting glyoxylate,⁶² a
10
11 435 proposed product of aerobic PEG chain shortening.³⁴ Genes participating in oxic and anoxic
12
13 436 transformations of glyoxylate were also predicted in the samples (K01638/EC2.3.3.9,
14
15 437 K00015/EC1.1.1.26), suggesting that mineralization of these products may have occurred in the
16
17 438 microcosms.
18
19
20
21
22

439

440 **Implications of PEG and PPG degradation in groundwater**

23
24
25 441 Collectively, the predicted presence of genes associated with enzymatic pathways for the
26
27 442 aerobic degradation of PEGs, PPGs, and their metabolites combined with the identification of
28
29 443 mono- and di-carboxylated intermediate polyglycol products support the inference that PEG and
30
31 444 PPG removal during the oxic phase was largely due to biodegradation. These results
32
33 445 demonstrate the role that aerobic sediment microorganisms are likely to play in degrading PEG
34
35 446 and PPG polymers, with implications for disruption of the natural microbial community (i.e.,
36
37 447 lower diversity and/or enrichment of key taxa) in the event of a release of produced water to
38
39 448 shallow groundwater.
40
41
42
43

44 449 Given the persistence observed in our microcosms under anoxic conditions, PEGs and
45
46 450 PPGs are more likely to be detected at sites where anoxic conditions prevail. The degradation
47
48 451 products identified in our microcosms could help characterize releases of produced water to
49
50 452 shallow groundwater even when the parent compounds have been largely transformed. The
51
52 453 PPG-COOH product was persistent under both oxic and anoxic conditions (Figs. 5c and S15).
53
54 454 Both carboxylated PEG products appeared to be persistent under anoxic conditions; however,
55
56
57
58
59
60

1
2
3 455 PEG-COOH and PEG-diCOOH emerged and were both subsequently degraded during the longer
4
5 456 oxic periods in the A-611 and B-161 microcosms (Figs. 3c and S16). Thus, the PEG products
6
7
8 457 may not be detected at sites with stable or prolonged oxic conditions.
9

10 458 Produced water composition is heterogeneous between different wells, formations, and
11
12 459 production ages,⁸⁻¹¹ which could result in variable detection or degradation kinetics of PEGs and
13
14 460 PPGs. While the detection of PEGs and PPGs in the A-611 and B-161 samples demonstrates
15
16 461 that these compounds may be present long after well stimulation, the lower concentrations
17
18 462 require sensitive analytical methods to detect. We found that PPGs were more persistent in
19
20 463 produced waters with higher initial concentrations. We observed rapid PEG removal at the low
21
22 464 concentrations present in the produced water microcosms; however, half-lives reported for high
23
24 465 PEG concentrations, representative of initial hydraulic fracturing fluid composition, were an
25
26 466 order of magnitude longer.²⁸ Rosenblum et al.¹¹ showed that concentrations of PEGs and PPGs
27
28 467 in Denver-Julesburg Basin produced water decreased approximately 50% within the first two
29
30
31 468 weeks of production. Thus, PEGs and PPGs are more likely to be detected at sites with a release
32
33 469 shortly after production begins due to both higher initial concentrations and potentially slower
34
35 470 degradation rates.
36
37
38
39

40 471 Given the frequency of accidental surface spills associated with unconventional oil and
41
42 472 gas activities, there is a need to understand the natural attenuation rates and pathways of organic
43
44 473 constituents in the produced fluids. Our results demonstrate the differences between PEG and
45
46 474 PPG degradation rates and pathways. These insights may be utilized to better characterize
47
48 475 shallow groundwater contamination following a release of produced water.
49
50

51 476

52 477

1
2
3 478 **ASSOCIATED CONTENT**

4
5 479 **Supporting Information:** Additional detail on methods; MS-MS for PEG-diCOOH and
6
7
8 480 PPG-COOH products; 10 tables and 16 figures detailing compound identification, redox and
9
10 481 ATP results, and microbial community analysis.

11
12 482

13
14
15 483 **AUTHOR INFORMATION**

16
17 484 **Corresponding Author:** *E-mail: joseph.ryan@colorado.edu. Phone: (303)492-0772.

18
19 485

20
21
22 486 **CONFLICTS OF INTEREST**

23
24 487 There are no conflicts of interest to declare.

25
26 488

27
28
29 489 **ACKNOWLEDGEMENTS**

30
31 490 This research is supported by the AirWaterGas Sustainability Research Network funded by the
32
33 491 National Science Foundation (CBET-1240584) and the University of Colorado CEAE
34
35 492 Department Doctoral Assistantship for Completion of Dissertation. P.J.M. and M.V.E. were
36
37
38 493 partially supported by NSF CBET award no. 1823069. We thank Katherine Armstrong for
39
40 494 assistance with sampling, Dr. Fred Luiszer for assistance with ICP-OES and IC analysis, and
41
42 495 Dr. Jerry Zweigenbaum (Agilent Technologies) for support of our UHPLC/qTOF-MS
43
44
45 496 instrumentation. We also thank our industry collaborator for providing access and assistance with
46
47 497 produced water collection.

48
49 498

50
51 499

52
53
54 500

55

56

57

58

59

60

501

REFERENCES

- (1) J. L. Adgate, B. D. Goldstein and L. M. McKenzie, Potential public health hazards, exposures and health effects from unconventional natural gas development, *Environmental Science & Technology*, 2014, **48**, 8307-8320.
- (2) A. Vengosh, R. B. Jackson, N. Warner, T. H. Darrah and A. Kondash, A critical review of the risks to water resources from unconventional shale gas development and hydraulic fracturing in the United States, *Environmental Science & Technology*, 2014, **48**, 8334-8348.
- (3) R. D. Vidic, S. L. Brantley, J. M. Vandenbossche, D. Yoxheimer and J. D. Abad, Impact of shale gas development on regional water quality, *Science*, 2013, **340**.
- (4) W. T. Stringfellow, J. K. Domen, M. K. Camarillo, W. L. Sandelin and S. Borglin, Physical, chemical, and biological characteristics of compounds used in hydraulic fracturing, *Journal of Hazardous Materials*, 2014, **275**, 37-54.
- (5) I. Ferrer and E. M. Thurman, Chemical constituents and analytical approaches for hydraulic fracturing waters, *Trends in Environmental Analytical Chemistry*, 2015, **5**, 18-25.
- (6) M. Elsner and K. Hoelzer, Quantitative survey and structural classification of hydraulic fracturing chemicals reported in unconventional gas production, *Environmental Science & Technology*, 2016, **50**, 3290-3314.
- (7) A. Butkovskiy, H. Bruning, S. A. E. Kools, H. H. M. Rijnaarts and A. P. Van Wezel, Organic pollutants in shale gas flowback and produced waters: Identification, potential ecological impact, and implications for treatment strategies, *Environmental Science & Technology*, 2017, **51**, 4740-4754.
- (8) K. Oetjen, C. Danforth, M. C. McLaughlin, M. Nell, J. Blotevogel, D. E. Helbling, D. Mueller and C. P. Higgins, Emerging analytical methods for the characterization and quantification of organic contaminants in flowback and produced water, *Trends in Environmental Analytical Chemistry*, 2017.
- (9) J. L. Luek and M. Gonsior, Organic compounds in hydraulic fracturing fluids and wastewaters: A review, *Water Research*, 2017, **123**, 536-548.
- (10) W. Orem, C. Tatu, M. Varonka, H. Lerch, A. Bates, M. Engle, L. Crosby and J. McIntosh, Organic substances in produced and formation water from unconventional natural gas extraction in coal and shale, *International Journal of Coal Geology*, 2014, **126**, 20-31.
- (11) J. Rosenblum, E. M. Thurman, I. Ferrer, G. Aiken and K. G. Linden, Organic chemical characterization and mass balance of a hydraulically fractured well: From fracturing fluid to produced water over 405 days, *Environmental Science & Technology*, 2017, **51**, 14006-14015.
- (12) B. D. Drollette, K. Hoelzer, N. R. Warner, T. H. Darrah, O. Karatum, M. P. O'Connor, R. K. Nelson, L. A. Fernandez, C. M. Reddy, A. Vengosh, R. B. Jackson, M. Elsner and D. L. Plata, Elevated levels of diesel range organic compounds in groundwater near Marcellus gas operations are derived from surface activities, *Proceedings of the National Academy of Sciences of the United States of America*, 2015, **112**, 13184-13189.
- (13) S. A. Gross, H. J. Avens, A. M. Banducci, J. Sahmel, J. M. Panko and B. E. Tvermoes, Analysis of BTEX groundwater concentrations from surface spills associated with hydraulic fracturing operations, *Journal of the Air & Waste Management Association*, 2013, **63**, 424-432.

- 1
2
3 545 (14) G. T. Llewellyn, F. Dorman, J. L. Westland, D. Yoxtheimer, P. Grieve, T. Sowers, E.
4 546 Humston-Fulmer and S. L. Brantley, Evaluating a groundwater supply contamination
5 547 incident attributed to Marcellus Shale gas development, *Proceedings of the National*
6 548 *Academy of Sciences of the United States of America*, 2015, **112**, 6325-6330.
- 8 549 (15) K. J. Armstrong, J. D. Rogers, T. L. Burke and J. N. Ryan, Characterization of accidental
9 550 spills and releases affecting groundwater in the Greater Wattenburg Area of the Denver-
10 551 Julesburg Basin in northeastern Colorado, In *SPE Health, Safety, Security, Environment, &*
11 552 *Social Responsibility Conference - North America*, Society of Petroleum Engineers, New
12 553 Orleans, Louisiana, 18-20 April 2017, 2017.
- 14 554 (16) K. O. Maloney, S. Baruch-Mordo, L. A. Patterson, J. P. Nicot, S. A. Entekin, J. E.
15 555 Fargione, J. M. Kiesecker, K. E. Konschnik, J. N. Ryan, A. M. Trainor, J. E. Saiers and H. J.
16 556 Wiseman, Unconventional oil and gas spills: Materials, volumes, and risks to surface waters
17 557 in four states of the US, *Science of the Total Environment*, 2017, **581**, 369-377.
- 18 558 (17) S. Burden, M. A. Cluff, L. E. DeHaven, C. Roberts, S. L. Sharkley and A. Singer, *Review of*
19 559 *State and Industry Spill Data: Characterization of Hydraulic Fracturing-Related Spills*,
20 560 EPA/601/R-14/001, U.S. Environmental Protection Agency Office of Research and
21 561 Development: Washington, D.C., 2015.
- 23 562 (18) E. M. Thurman, I. Ferrer, J. Blotvogel and T. Borch, Analysis of hydraulic fracturing
24 563 flowback and produced waters using accurate mass: Identification of ethoxylated surfactants,
25 564 *Analytical Chemistry*, 2014, **86**, 9653-9661.
- 26 565 (19) E. M. Thurman, I. Ferrer, J. Rosenblum, K. Linden and J. N. Ryan, Identification of
27 566 polypropylene glycols and polyethylene glycol carboxylates in flowback and produced water
28 567 from hydraulic fracturing, *Journal of Hazardous Materials*, 2017, **323**, 11-17.
- 30 568 (20) Y. H. He, S. L. Flynn, E. J. Folkerts, Y. F. Zhang, D. L. Ruan, D. S. Alessi, J. W. Martin
31 569 and G. G. Goss, Chemical and toxicological characterizations of hydraulic fracturing
32 570 flowback and produced water, *Water Research*, 2017, **114**, 78-87.
- 33 571 (21) K. Oetjen, K. E. Chan, K. Gulmark, J. H. Christensen, J. Blotvogel, T. Borch, J. R. Spear,
34 572 T. Y. Cath and C. P. Higgins, Temporal characterization and statistical analysis of flowback
35 573 and produced waters and their potential for reuse, *Science of the Total Environment*, 2018,
36 574 **619-620**, 654-664.
- 38 575 (22) M. Nell and D. E. Helbling, Exploring matrix effects and quantifying organic additives in
39 576 hydraulic fracturing associated fluids using liquid chromatography electrospray ionization
40 577 mass spectrometry, *Environmental Science: Processes & Impacts*, 2018, DOI:
41 578 10.1039/C8EM00135A.
- 42 579 (23) J. D. Rogers, T. L. Burke, S. G. Osborn and J. N. Ryan, A framework for identifying
43 580 organic compounds of concern in hydraulic fracturing fluids based on their mobility and
44 581 persistence in groundwater, *Environmental Science & Technology Letters*, 2015, **2**, 158-164.
- 46 582 (24) P. J. Mouser, S. Liu, M. A. Cluff, M. McHugh, J. J. Lenhart and J. D. MacRae, Redox
47 583 conditions alter biodegradation rates and microbial community dynamics of hydraulic
48 584 fracturing fluid organic additives in soil-groundwater microcosms. *Environmental*
49 585 *Engineering Science*, 2016, **33**.
- 50 586 (25) D. Kekacs, B. D. Drollette, M. Brooker, D. L. Plata and P. J. Mouser, Aerobic
51 587 biodegradation of organic compounds in hydraulic fracturing fluids, *Biodegradation*, 2015,
52 588 **26**, 271-287.
53 589
54
55
56
57
58
59
60

- 1
2
3 590 (26) J. D. Rogers, I. Ferrer, S. S. Tummings, A. Bielefeldt and J. N. Ryan, Inhibition of
4 591 biodegradation of hydraulic fracturing compounds by glutaraldehyde: Groundwater column
5 592 and microcosm experiments, *Environmental Science and Technology*, 2017, **51**, 10251-
6 593 10261.
- 7
8 594 (27) L. C. Strong, T. Gould, L. Kasinkas, M. J. Sadowsky, A. Aksan and L. P. Wackett,
9 595 Biodegradation in waters from hydraulic fracturing: Chemistry, microbiology, and
10 596 engineering, *Journal of Environmental Engineering*, 2014, **140**.
- 11 597 (28) M. C. McLaughlin, T. Borch and J. Blotvogel, Spills of hydraulic fracturing chemicals on
12 598 agricultural topsoil: Biodegradation, sorption, and co-contaminant interactions,
13 599 *Environmental Science & Technology*, 2016, **50**, 6071-6078.
- 14 600 (29) A. Zgola-Grzeskowiak, T. Grzeskowiak, J. Zembrzuska and Z. Lukaszewski, Comparison
15 601 of biodegradation of poly(ethylene glycol)s and poly(propylene glycol)s, *Chemosphere*,
16 602 2006, **64**, 803-809.
- 17
18 603 (30) M. Bernhard, J. P. Eubeler, S. Zok and T. P. Knepper, Aerobic biodegradation of
19 604 polyethylene glycols of different molecular weights in wastewater and seawater, *Water*
20 605 *Research*, 2008, **42**, 4791-4801.
- 21
22 606 (31) E. Beran, S. Hull and M. Steininger, The relationship between the chemical structure of
23 607 poly(alkylene glycol)s and their aerobic biodegradability in an aqueous environment, *Journal*
24 608 *of Polymers and the Environment*, 2013, **21**, 172-180.
- 25 609 (32) A. Zgola-Grzeskowiak, T. Grzeskowiak, J. Zembrzuska, M. Franska, R. Franski, T. Kozik
26 610 and Z. Lukaszewski, Biodegradation of poly(propylene glycol)s under the conditions of the
27 611 OECD screening test, *Chemosphere*, 2007, **67**, 928-933.
- 28
29 612 (33) R. J. West, J. W. Davis, L. H. Pottenger, M. I. Banton and C. Graham, Biodegradability
30 613 relationships among propylene glycol substances in the organization for economic
31 614 cooperation and development ready- and seawater biodegradability tests, *Environmental*
32 615 *Toxicology and Chemistry*, 2007, **26**, 862-871.
- 33 616 (34) F. Kawai, Microbial degradation of polyethers, *Applied Microbiology and Biotechnology*,
34 617 2002, **58**, 30-38.
- 35 618 (35) J. P. Eubeler, M. Bernhard and T. P. Knepper, Environmental biodegradation of synthetic
36 619 polymers II. Biodegradation of different polymer groups, *Trends in Analytical Chemistry*,
37 620 2010, **29**, 84-100.
- 38
39 621 (36) K. M. Heyob, J. Blotvogel, M. Brooker, M. V. Evans, J. J. Lenhart, J. Wright, R.
40 622 Lamendella, T. Borch and P. J. Mouser, Natural attenuation of nonionic surfactants used in
41 623 hydraulic fracturing fluids: Degradation rates, pathways, and mechanisms, *Environmental*
42 624 *Science & Technology*, 2017, **51**, 13985-13994.
- 43 625 (37) S. Wagener and B. Schink, Fermentative degradation of nonionic surfactants and
44 626 polyethylene-glycol by enrichment cultures and by pure cultures of homoacetogenic and
45 627 propionate-forming bacteria, *Applied and Environmental Microbiology*, 1988, **54**, 561-565.
- 46
47 628 (38) D. F. Dwyer and J. M. Tiedje, Metabolism of polyethylene glycol by two anaerobic
48 629 bacteria, *Desulfovibrio Desulfuricans* and a *Bacteroides sp*, *Applied and Environmental*
49 630 *Microbiology*, 1986, **52**, 852-856.
- 50 631 (39) S. S. Paschke, ed, *Groundwater Availability of the Denver Basin Aquifer System, Colorado*,
51 632 Professional Paper 1770, U.S. Geological Survey: Reston, Va., 2011.
- 52
53 633 (40) American Public Health Association, American Water Works Association, Water
54 634 Environment Federation, *Standard Methods for the Examination of Water and Wastewater*,
55 635 United Book Press, Inc, Baltimore, MD, 20th edn., 1998.
- 56
57
58
59
60

- 1
2
3 636 (41) Earth Microbiome Project, 16S Illumina Amplicon Protocol,
4 637 <http://press.igsb.anl.gov/earthmicrobiome/protocols-and-standards/16s/>, (accessed Aug
5 638 2017).
6
7 639 (42) J. G. Caporaso, J. Kuczynski, J. Stombaugh, K. Bittinger, F. D. Bushman, et al., QIIME
8 640 allows analysis of high-throughput community sequencing data, *Nature Methods*, 2010, **7**,
9 641 335-336.
10 642 (43) Ohio Supercomputer Center, 1987.
11 643 (44) T. Z. DeSantis, P. Hugenholtz, N. Larsen, M. Rojas, E. L. Brodie, K. Keller, T. Huber, D.
12 644 Dalevi, P. Hu and G. L. Andersen, Greengenes, a chimera-checked 16S rRNA gene database
13 645 and workbench compatible with ARB, *Applied and Environmental Microbiology*, 2006, **72**,
14 646 5069-5072.
15
16 647 (45) S. F. Altschul, W. Gish, W. Miller, E. W. Myers and D. J. Lipman, Basic local alignment
17 648 search tool, *Journal of Molecular Biology*, 1990, **215**, 403-410.
18 649 (46) M. G. Langille, J. Zaneveld, J. G. Caporaso, D. McDonald, D. Knights, et al., Predictive
19 650 functional profiling of microbial communities using 16S rRNA marker gene sequences,
20 651 *Nature Biotechnology*, 2013, **31**, 814-821.
21
22 652 (47) R. Caspi, R. Billington, L. Ferrer, H. Foerster, C. A. Fulcher, et al., The MetaCyc database
23 653 of metabolic pathways and enzymes and the BioCyc collection of pathway/genome
24 654 databases. *Nucleic Acids Research*, 2016, **44**, D471-480.
25 655 (48) P. J. Mouser, A. L. N'Guessan, H. Elifantz, D. E. Holmes, K. H. Williams, M. J. Wilkins, P.
26 656 E. Long and D. R. Lovley, Influence of heterogeneous ammonium availability on bacterial
27 657 community structure and the expression of nitrogen fixation and ammonium transporter
28 658 genes during in situ bioremediation of uranium-contaminated groundwater, *Environmental*
29 659 *Science & Technology*, 2009, **43**, 4386-4392.
30
31 660 (49) Groundwater Protection Council, Interstate Oil & Gas Conservation Commission,
32 661 FracFocus Chemical Disclosure Registry, <http://fracfocus.org>, (accessed May 2017).
33 662 (50) J. F. Gao, L. B. M. Ellis and L. P. Wackett, The University of Minnesota
34 663 biocatalysis/biodegradation database: Improving public access, *Nucleic Acids Research*,
35 664 2010, **38**, D488-D491.
36
37 665 (51) E. Otal and J. Lebrato, Anaerobic degradation of polyethylene glycol mixtures, *Journal of*
38 666 *Chemical Technology and Biotechnology*, 2003, **78**, 1075-1081.
39 667 (52) Y. L. Huang, Q. B. Li, X. Deng, Y. H. Lu, X. K. Liao, M. Y. Hong and Y. Wang, Aerobic
40 668 and anaerobic biodegradation of polyethylene glycols using sludge microbes, *Process*
41 669 *Biochemistry*, 2005, **40**, 207-211.
42 670 (53) F. Kawai, The biochemistry and molecular biology of xenobiotic polymer degradation by
43 671 microorganisms, *Bioscience, Biotechnology, and Biochemistry*, 2010, **74**, 1743-1759.
44 672 (54) M. Kanehisa, Y. Sato, M. Kawashima, M. Furumichi and M. Tanabe, KEGG as a reference
45 673 resource for gene and protein annotation, *Nucleic Acids Research*, 2016, **44**, D457-462.
46 674 (55) R. A. Daly, M. A. Borton, M. J. Wilkins, D. W. Hoyt, D. J. Kountz, et al, Microbial
47 675 metabolisms in a 2.5-km-deep ecosystem created by hydraulic fracturing in shales, *Nature*
48 676 *Microbiology*, 2016, **1**.
49
50 677 (56) M. A. Cluff, A. Hartsock, J. D. MacRae, K. Carter and P. J. Mouser, Temporal changes in
51 678 microbial ecology and geochemistry in produced water from hydraulically fractured
52 679 Marcellus Shale gas wells, *Environmental Science & Technology*, 2014, **48**, 6508-6517.
53 680
54
55
56
57
58
59
60

- 1
2
3 681 (57) J. Fichter, K. Wunch, R. Moore, E. Summer, S. Braman and P. Holmes, How Hot is Too
4 682 Hot for Bacteria? A Technical Study Assessing Bacterial Establishment in Downhole
5 683 Drilling, Fracturing and Stimulation Operations, In *NACE International Corrosion*
6 684 *Conference*, National Association of Corrosion Engineers International, Salt Lake City, UT,
7 685 March 11-15, 2012.
- 9 686 (58) V. M. Pathak and Navneet, Review on the current status of polymer degradation: A
10 687 microbial approach, *Bioresources and Bioprocessing*, 2017, **1**.
- 11 688 (59) N. Obradors and J. Aguilar, Efficient biodegradation of high-molecular-weight polyethylene
12 689 glycols by pure cultures of *Pseudomonas stutzeri*, *Applied and Environmental Microbiology*,
13 690 1991, **57**, 2383-2388.
- 15 691 (60) M. Sugimoto, M. Tanabe, M. Hataya, S. Enokibara, J. A. Duine and F. Kawai, The first step
16 692 in polyethylene glycol degradation by sphingomonads proceeds via a flavoprotein alcohol
17 693 dehydrogenase containing flavin adenine dinucleotide, *Journal of Bacteriology*, 2001, **183**,
18 694 6694-6698.
- 19 695 (61) R. Marchal, E. Nicolau and J. P. Ballaguet, Biodegradability of polyethylene glycol 400 by
20 696 complete microfloras, *International Biodeterioration & Biodegradation*, 2008, **62**, 384-390.
- 22 697 (62) C. Han, R. Mwirichia, O. Chertkov, B. Held, A. Lapidus, et al., Complete genome sequence
23 698 of *Syntrophobotulus glycolicus* type strain (FIGlyR), *Standards in Genomic Sciences*, 2011,
24 699 **4**, 371-380.
- 25 700
26
27
28
29
30
31
32
33
34
35
36
37
38
39
40
41
42
43
44
45
46
47
48
49
50
51
52
53
54
55
56
57
58
59
60

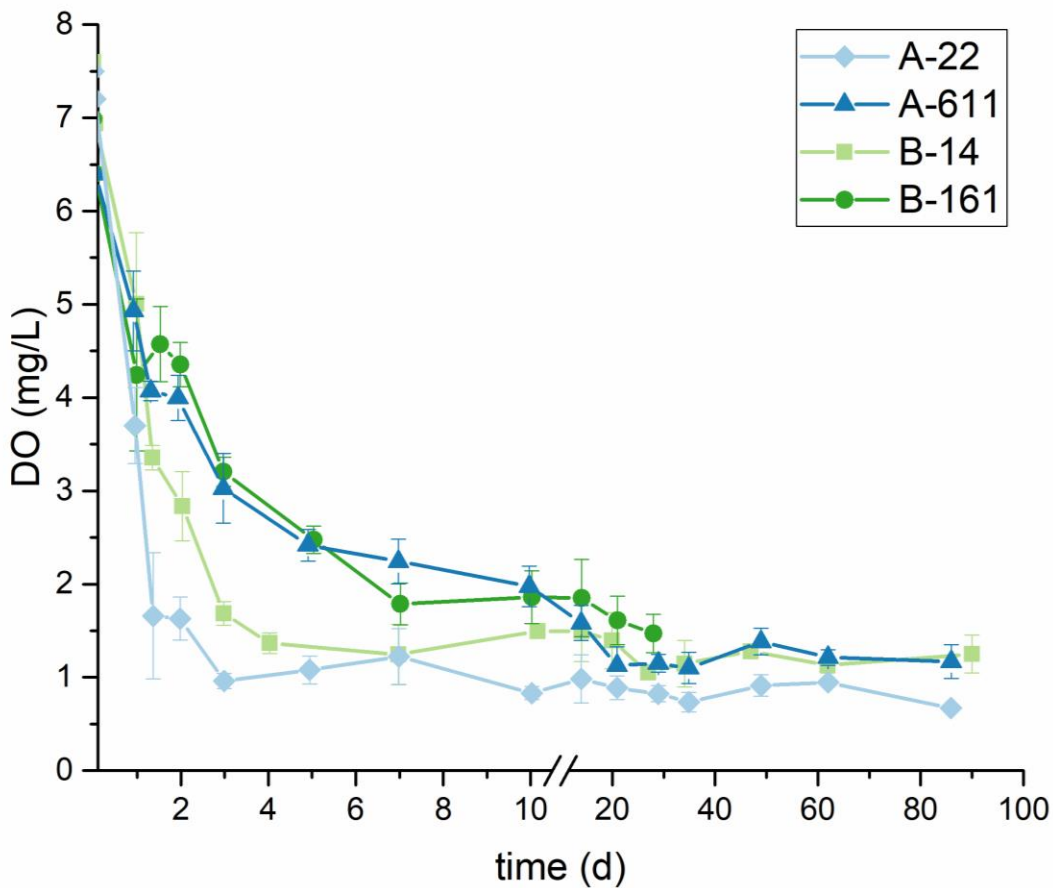
701 **Table 1.** Pseudo-first-order half-lives ($t_{1/2}$) and standard error fit during the oxic period of the
 702 produced water microcosm experiments.

microcosm	PEG-9 $t_{1/2}$ (d)	PPG-6 $t_{1/2}$ (d)
A-22	0.4 ± 0.1	7.5 ± 5.2
A-611	< 0.4	2.7 ± 0.5
B-14	1.1 ± 0.2	14 ± 3.7
B-161	< 0.4	2.5 ± 0.2

703

704

705 **Figure 1.** Dissolved oxygen (DO) vs. time in the A-22 (diamond symbols), A-611 (triangles),
 706 B-14 (squares), and B-161 (circles) microcosm experiments.



707

708

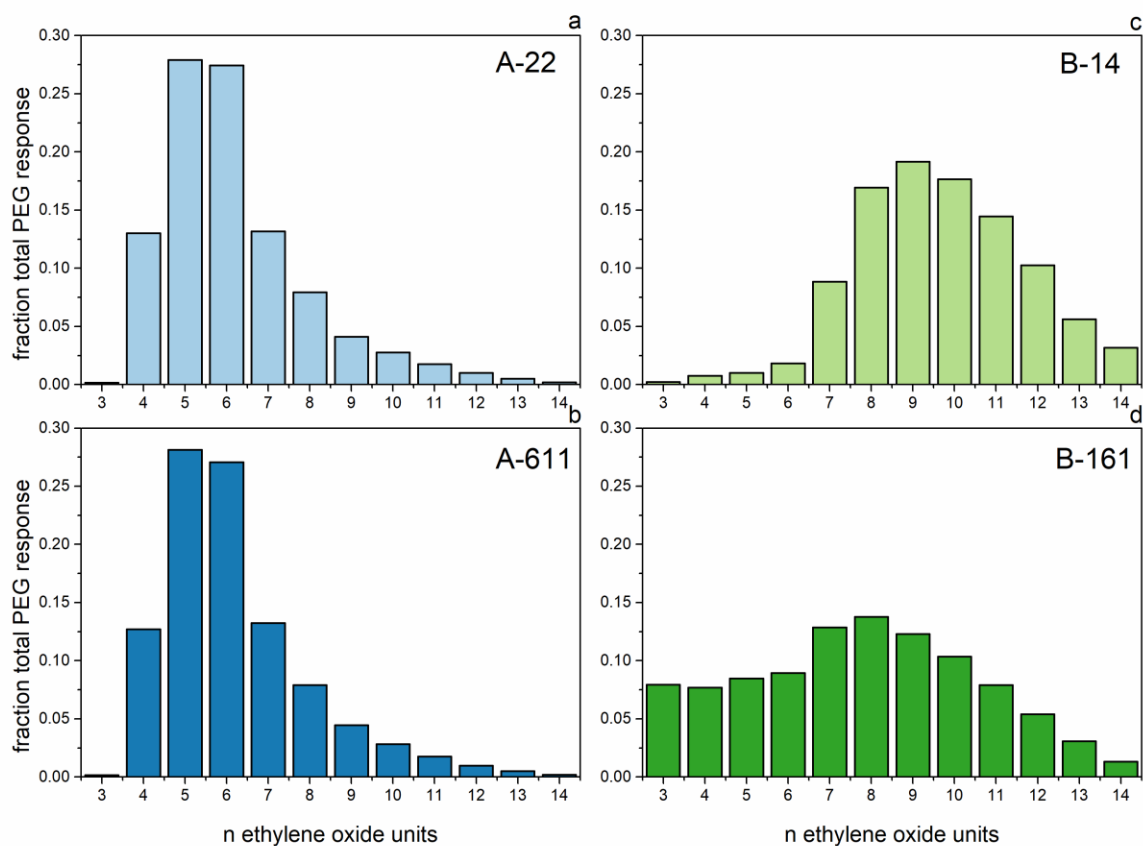
709

710

711

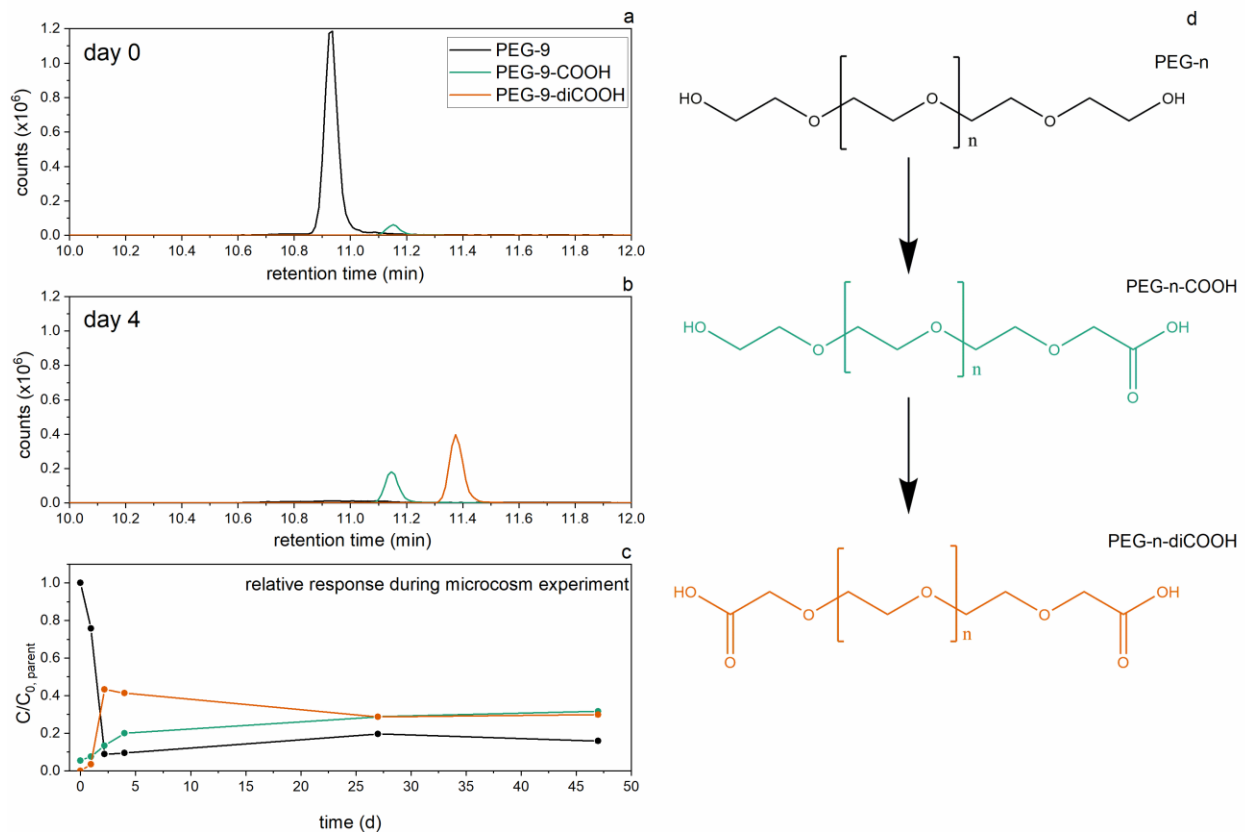
712

1
2
3 **708 Figure 2.** Initial (day 0) distribution of PEG homologues in (a) A-22, (b) A-611, (c) B-14, and
4
5 **709** (d) B-161 microcosms.
6
7



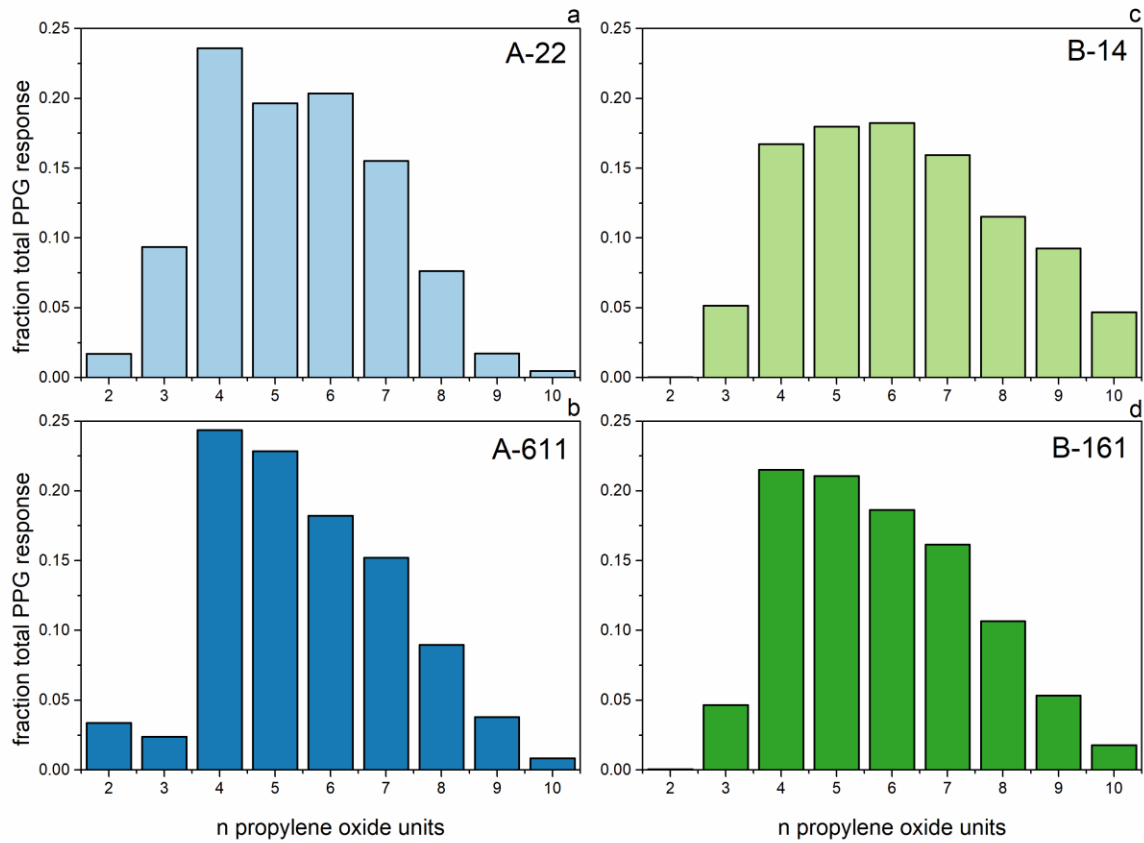
710
34
35
36
37
38
39
40
41
42
43
44
45
46
47
48
49
50
51
52
53
54
55
56
57
58
59
60

1
2
3 711 **Figure 3.** Chromatographic separation of PEG-9 (black trace) and corresponding products
4
5 712 PEG-9-COOH (green trace) and PEG-9-diCOOH (orange trace) on (a) day 0 and (b) day 4 of the
6
7 713 B-14 microcosm experiment, and (c) response (integrated peak area) of the three compounds
8
9 714 relative to PEG-9 ($C/C_{0,parent}$) during the microcosm experiment. The aerobic metabolic pathway
10
11 715 is shown (d).

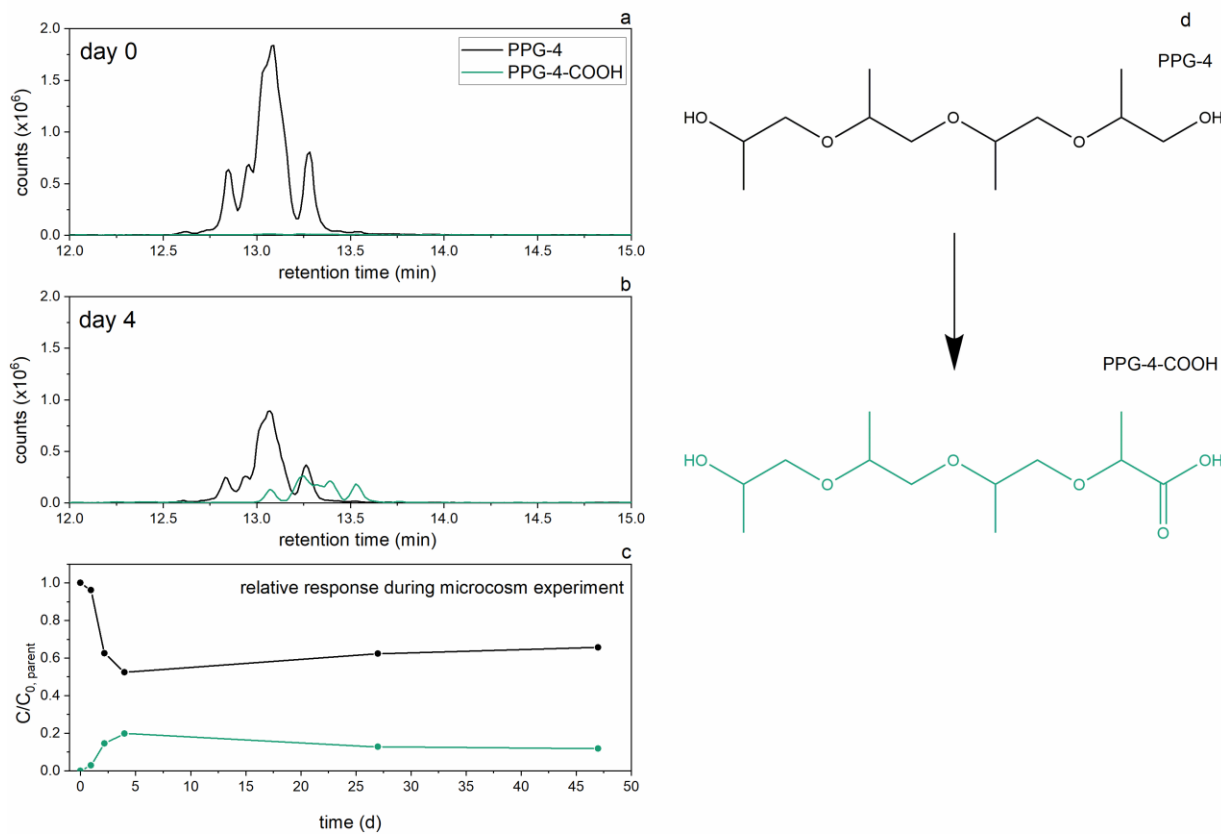


716
717

1
2
3 **718 Figure 4.** Initial (day 0) distribution of PPG homologues in (a) A-22, (b) A-611, (c) B-14, and
4
5 **719** (d) B-161 microcosms.
6
7



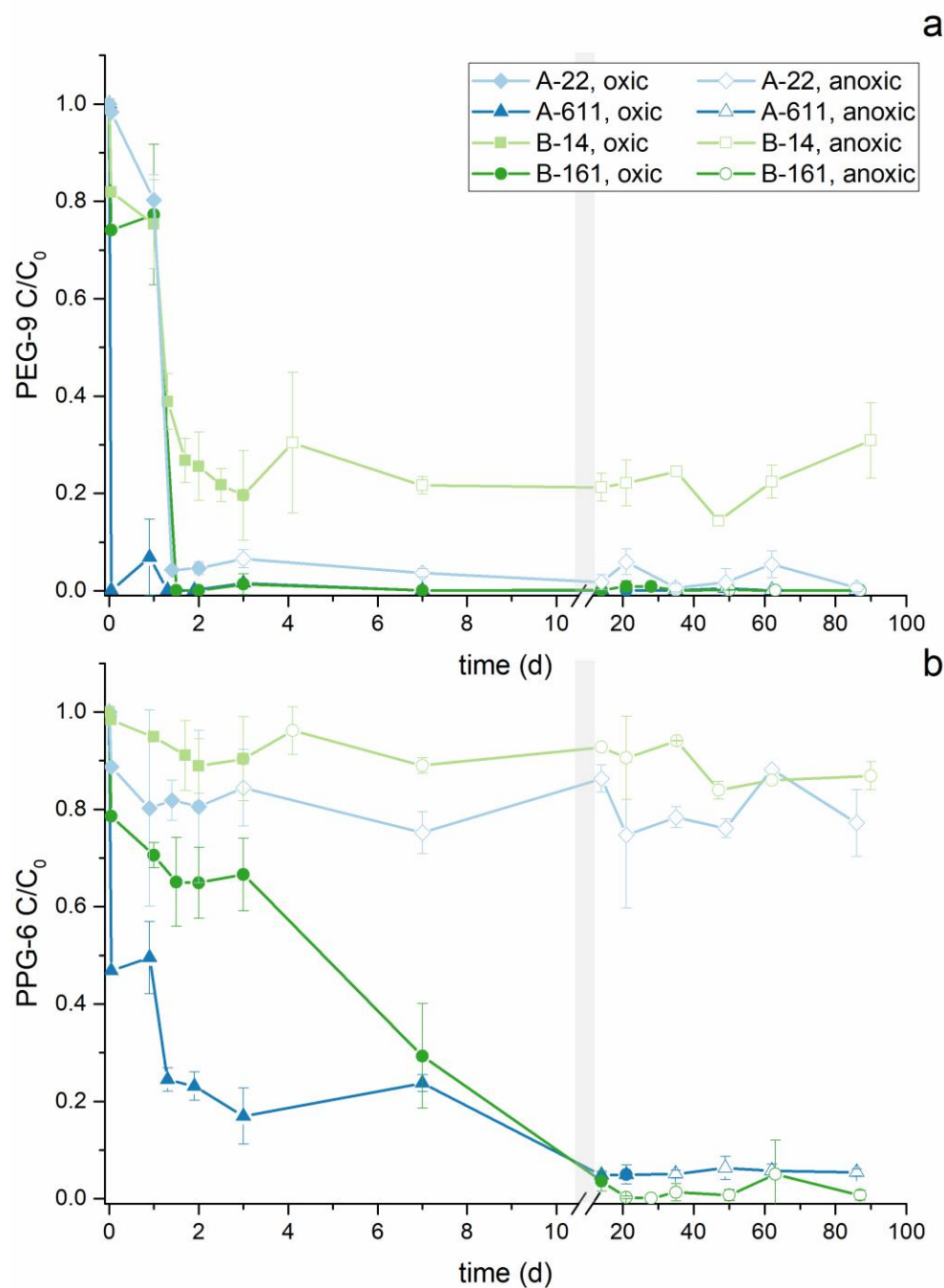
1
2
3 722 **Figure 5.** Chromatographic separation of PPG-4 (black trace) and corresponding product
4
5 723 PPG-4-COOH (green trace) on (a) day 0 and (b) day 4 of the B-14 microcosm experiment, and
6
7
8 724 (c) response (integrated peak area) of the three compounds relative to PPG-4 ($C/C_{0,parent}$) during
9
10 725 the microcosm experiment. The aerobic metabolic pathway is shown (d).



726

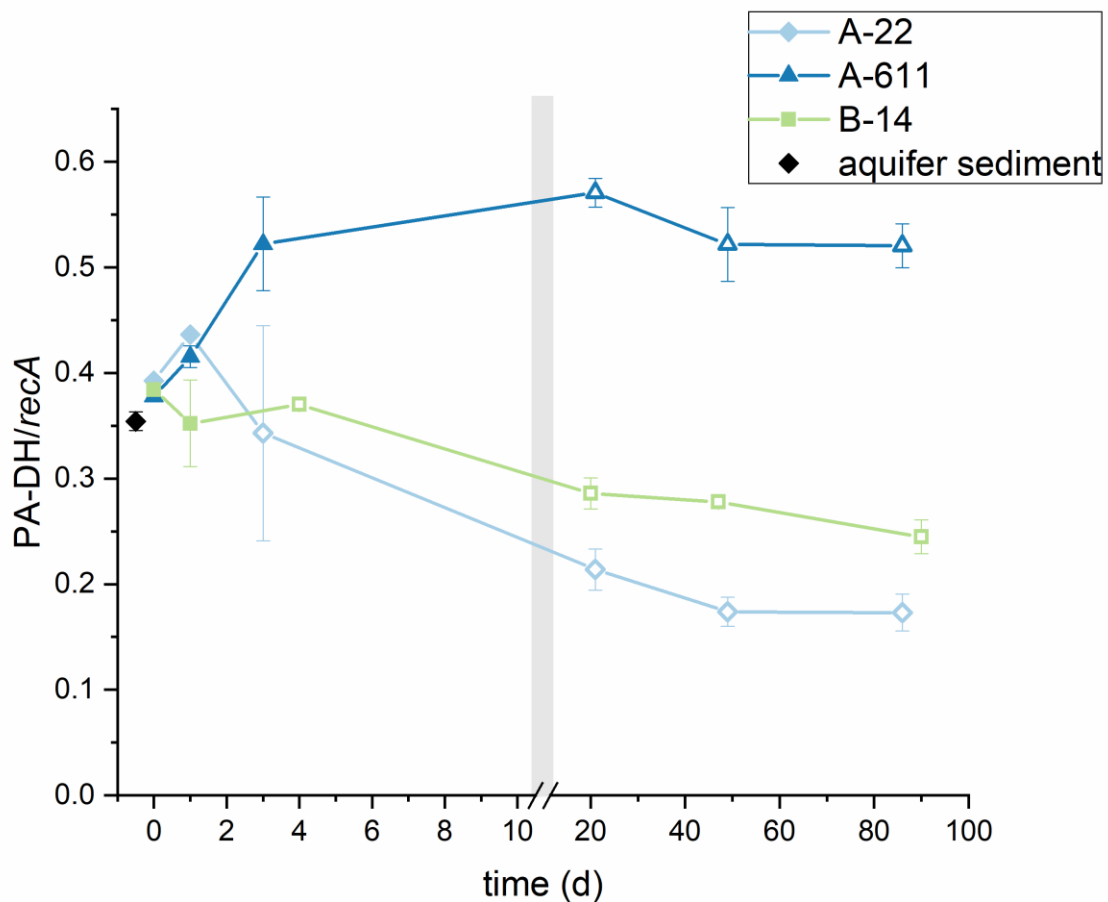
727

1
2
3 **728 Figure 6.** Degradation of (a) PEG-9 and (b) PPG-6 in A-22 (diamond symbols), A-611
4 (triangles), B-14 (squares), and B-161 (circles) microcosms. Oxic and anoxic periods are
5 729 represented by solid and open symbols, respectively. An axis break at day 10 is used to show
6 730 detail for rapid degradation.
7
8
9
10 731 detail for rapid degradation.



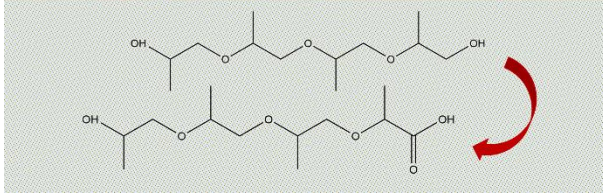
732

1
2
3 733 **Figure 7.** Abundance of the primary alcohol dehydrogenase gene (PA-DH) relative to a
4
5 734 housekeeping gene (*recA*) generated from metagenomes predicted from the 16S rRNA gene of
6
7 735 microbial communities in the A-22 (diamond symbols), A-611 (triangles), and B-14 (squares)
8
9 736 microcosms, in addition to the aquifer sediment prior to exposure to produced water (black
10
11 737 diamond symbol). Oxidic and anoxic periods are represented by solid and open symbols,
12
13 738 respectively.



739

740

741 **Table of Contents Graphic**

742

743

744 Polyethylene glycol, polypropylene glycol, and their degradation products could be utilized to
745 better characterize shallow groundwater contamination following a spill of produced water.

1
2
3
4
5
6
7
8
9
10
11
12
13
14
15
16
17
18
19
20
21
22
23
24
25
26
27
28
29
30
31
32
33
34
35
36
37
38
39
40
41
42
43
44
45
46
47
48
49
50
51
52
53
54
55
56
57
58
59
60